

# Experimental Investigation of the Flapping Performance on ‘Delfly Micro’

S. Deng, B.W.vanOudheusden, B.D.W.Remes, M.Percin, H.Bijl and H.M.Ruijsink

Delft University of Technology, Delft, the Netherlands  
S.Deng@tudelft.nl

## Abstract

This study addresses the quantification of the aerodynamic performance of the ‘Delfly Micro’, which is currently the smallest ornithopter in the ‘Delfly’ family with an X-Wing configuration. Aerodynamic forces were measured on a full-scale ‘Delfly Micro’ by a sophisticated balance system. In view of the influence of the wing flexibility on the performance, wings with varying membrane thicknesses and stiffener orientations were examined in hovering case. To characterize the forward flight regime, aerodynamic forces were also measured with varying free stream velocities and angles of attack in wind tunnel. The results indicate that wing flexibility indeed influences the aerodynamic performance, where a more rigid wing can produce more force, whereas with a lower force to power ratio. According to the wind tunnel data, the ‘Delfly Micro’ can attain a flight speed up to 3 m/s, at a flapping frequency over 30 Hz and angle of attack of 30 degrees.

## 1 Introduction

FMAVs (flapping wing Micro Air Vehicles) have gained interest due to their potential in flight efficiency and maneuverability. Since 2005, the MAV group at Delft University of Technology has engaged in the development and research of FMAVs regarding the related technologies in aerodynamics, mechanism, electronics and autonomy, etc. Our group has developed three types of ornithopters different in size: ‘Delfly I’, ‘Delfly II’ and ‘Delfly Micro’. It is the Delfly development philosophy to keep minimizing the size of the Delfly without sacrificing the flight performance. Previous studies [1, 2, 3, 4, 5] during the past years have focused on ‘Delfly II’. In this paper, we turn the attention to the smaller ‘Delfly Micro’, which only weighs 3 grams and has 10 cm wing span. With a 30mAh lithium polymer battery, it can fly for 3 minutes with a 50 m range. This small size makes it the smallest flying ornithopter with onboard camera in the world. Furthermore, the ‘Delfly Micro’ is an ideal platform for studying the aerodynamics of low Reynolds flyers in nature.

In this study, experiments on the aerodynamic performance of the real scale of ‘Delfly Micro’ have been conducted to obtain information on the preliminary flight envelop, including hovering and level flight. Flexibility of the wing significantly effects the overall aerodynamic performance of FMAV, as has been shown for Delfly II [5]. Therefore, three different membrane thicknesses (2, 5 and 10 micrometer) and three different stiffener layouts are examined under hovering flight conditions. A high speed camera is placed in front of the ‘Delfly Micro’ to detect the real-time phase angle during the flapping motion. The information from these images allow the aerodynamic forces to be synchronized with the corresponding wing position, hence, the phase in the flapping cycle. Further measurements are carried out to characterize the level flight with oncoming free stream. The wind velocity and angle of attack are varied between  $2 \sim 4 \text{ m/s}$  and  $20^\circ \sim 40^\circ$ , respectively. The forces and frequency detector signal are recorded instantaneously by the FPGA system, together with the motor current and voltage, to determine the power input.

This paper is organized as follows. In section 2 the experimental setup is presented. Subsequently, the results of the experimental and its analysis are described in section 3, followed by conclusion in section 4.

## 2 Experimental Setup

### 2.1 Full-scale ‘Delfly Micro’ Model and Force Sensor

In order to mimic the real flight performance of the ‘Delfly Micro’, the model we used is a 1:1 scaled model, as shown in Fig. (1Left)). Clap-and-fling had been proven as one of the high lift mechanisms in flapping wing flyers[6]. In order to generate more force during flight, ‘Delfly Micro has a flapping angle of  $120^\circ$  which gives three clap-and-fling occurrences during a flapping cycle, at both sides and at the top. To obtain a more reliable and stable RPM operation during the measurement, the actual DelFly Micro motor is replaced by a brushed DC motor (diameter  $\phi = 7\text{mm}$ ) that is actuated by an external power supply. The flapping frequency is captured by an optical resistance mounted on both sides of the main gear.

The force sensor used is an ATI Nano17 Titanium, which is the smallest 6-axis sensor for commercial use and which can resolve down to 0.149 gram force without filtering. A DC motor is coupled to the force balance to give a precisely changeable angle of attack in the range of  $-15^\circ$  to  $35^\circ$ . The measured forces are used to compute the resultant vertical force ( $\text{Lift} = T \sin \alpha + N \cos \alpha$ ) and the resultant horizontal force ( $\text{Thrust} = T \cos \alpha - N \sin \alpha$ ) acting on ‘Delfly Micro’, see Fig (1Right)).

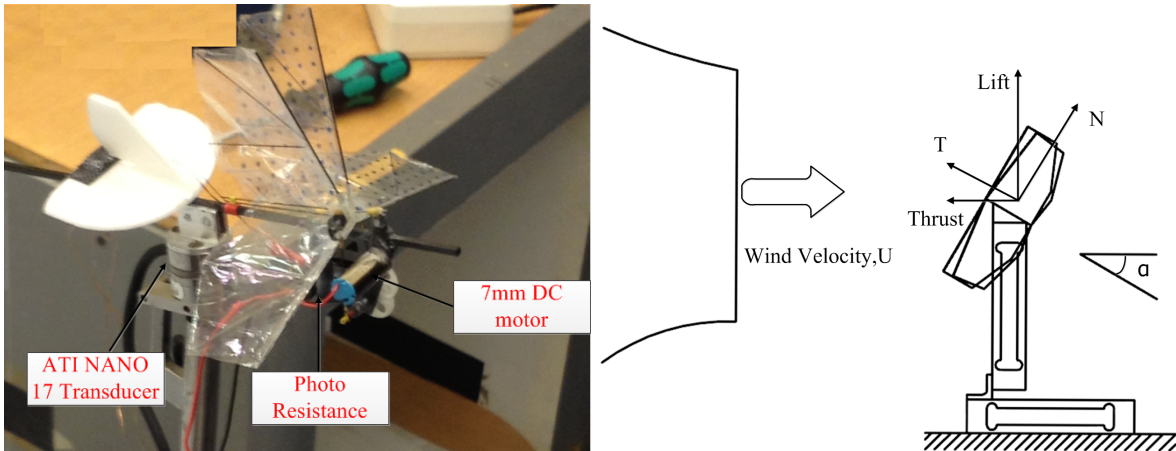


Figure 1: ‘Delfly Micro’ Model and its force relation on force balance. Left: ‘Delfly Micro’ Model; Right: Force on force balance.

### 2.2 Wind Tunnel

The measurements with free stream are conducted in the open jet W-Tunnel at the Delft University of Technology (DUT), shown in Fig.(2). The measurement section is a square section with  $0.6\text{m} \times 0.6\text{m}$ , which is large enough to prevent the jet shear layers’ interaction with ‘Delfly Micro’. The contraction

ratio is 3.62 and a maximum flow speed of around 15 m/s can be obtained[7]. In order to detect the incoming flow velocity, a calibrated hot wire velocity system is placed in the nozzle.

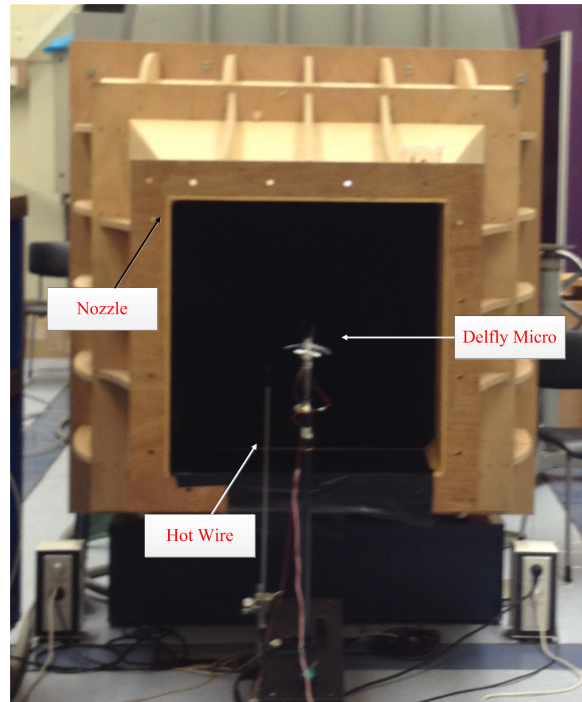


Figure 2: W-Tunnel in DUT

### 2.3 Wing Construction

Fig. 3 shows the standard wing layout used on ‘Delfly Micro’, with the wing span of 100 mm and aspect ratio of 3.2. The reason for choosing this configuration as the starting point is that such wing shape and stiffness orientation has been empirically optimized as the most efficient wing for the DelFly II[5].

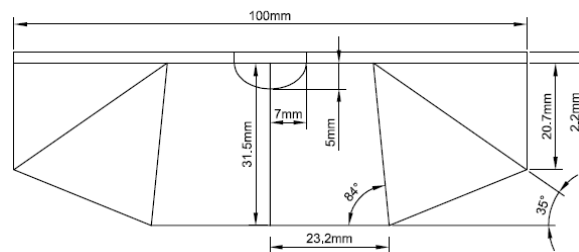

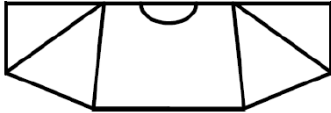
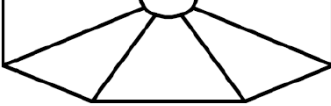


Figure 3: Schematics of ‘Delfly Micro’ Wing

In order to address the effect of flexibility on the wing, 6 sets of wings with varying membrane

thickness and stiffener orientation were built, as summarized in Table.1. The leading edge and stiffeners in all the wings are carbon rods with  $\phi=0.5\text{mm}$  and  $0.15\text{mm}$ , respectively. Furthermore, the wings are in-house built, following the technique developed by Bruggeman[5], using a vacuum table to guarantee the symmetry and uniform tension distribution on Mylar membrane.

Table. 1 Wing Properties

Name	Wing Layout
2_Clean	
5_Clean	
2_Std	
5_Std	
10_Std	
2_DiffStiff	
<p>Note: the first number in the name of the wings represents the Mylar thickness in <math>\mu\text{m}</math>. <b>Clean</b> indicates the wings without stiffeners <b>Std</b> is Standard Wing. <b>DiffStiff</b> is the wings with different stiffeners orientation.</p>	

### 3 Results

#### 3.1 Phase Distribution and Force Synchronization

To determine the phase distribution, i.e. the wing position variation over the flapping cycle, a high speed camera is placed in front of the Delfly Micro. 1000 images are taken at an acquisition frequency of 3000Hz. The Canny method is employed to detect the edges, because it is less sensitive to noise. The Hough transform is then applied to detect the leading edges in the binary images. The obtained phase distribution is fitted by a 6 order polynomial curve fit. Leading edge recognitions are performed on the 2\_Std Wing for different flapping frequencies, seen in Fig. (??). Aerodynamic forces are synchronized via locating the triggered signal for the camera from the optical sensor. Fig. (4(Right)) shows the synchronized forces corresponding to Fig. (4(Left)) for different frequencies. It can be observed that, when increasing the flapping frequency, the thrust production is increased. Furthermore, the peak in generated thrust shifts with the frequency, which had also be observed in the research of Delfly II[7].

The explanation of this shift phenomena is as yet not explained and remains an interesting topic for further investigation.

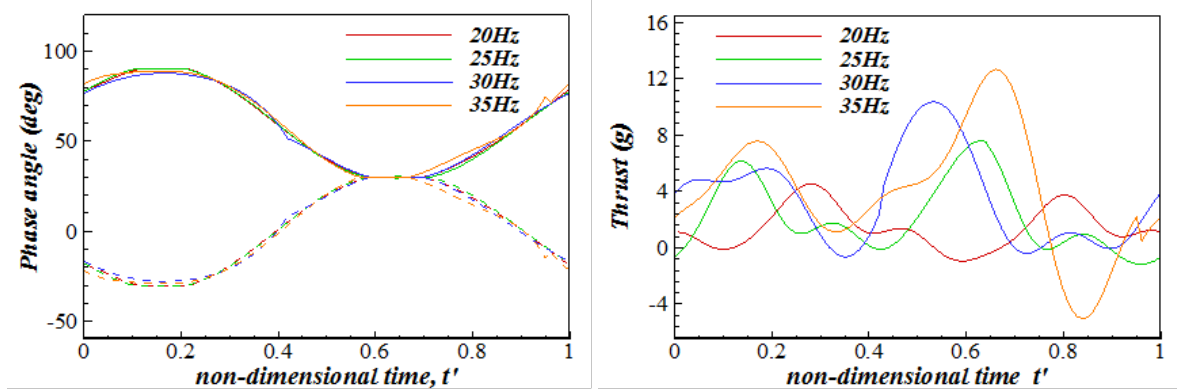


Figure 4: Phase distribution and force history during the flapping cycle. Left: Phase distribution of upper and lower wing, solid line is the leading edge of the upper wing, lower wing phase angle is represented with dashed line; Right: Forces from different flapping frequencies over the flapping cycle.

### 3.2 Effect of Wing Flexibility

Investigation of the influence of wing flexibility is conducted on the 6 sets of wings in Table.1. Thrust force is converted to grams and the power consumption can be obtained by Joules law  $P = I_{measured} \times V_{measured}$ . Furthermore, the ratio of thrust production to power consumption (T/P), which is a critical driving parameter in design optimization, is examined to evaluate the performance of the wings.

Tested results are plotted in Fig. (5). It can be seen that the clean wing configurations require the smallest power input when compared with the stiffened wings. However, the low thrust generated by the clean wing results in an inefficient configuration in view of the thrust to power ratio, as shown in Fig. (5(Right)). The wings with stiffeners and 5 and 10m Mylar foils produce almost the same thrust, at a given flapping frequency. Wing 2\_Std has a lower thrust production as may be expected from the increased amount of flexibility. Fig. (5(Middle)) illustrates that the more rigid wing required more power input respect to certain frequency. From Fig. (5(Right)), it follows that all the stiffened wings have better thrust to power ratio than the clean wings, and that Wing 2\_Std possesses the best performance. Wing 2\_DiffStiff displays the original wing stiffener configuration that has been used on the 'Delfly Micro' in the past, and which had also been examined in present test for comparison. One can see that this initial wing generates less thrust than the other stiffened wings. Meanwhile, it is more power consuming and a poor T/P performance of the 2\_DiffStiff wing results, as can be seen in Fig. (5(Right)). Overall, within the enveloped flapping frequency of 'Delfly Micro' regions from 25Hz to 35Hz, the standard wing built with a 2 m foil displays the best performance, in terms of the highest thrust to power ratio. Note that the thrust generated around 30Hz is around 3 grams, which is equal to the total weight of 'Delfly Micro'. That means 'Delfly Micro' is potentially able to hover. However, it has been observed that it cannot hover in real flight test, perhaps because the aerodynamic force and the weight distribution always produce a pitch moment in real flight. Further optimization has to be carried out on the current 'Delfly Micro' configuration to achieve hover ability.

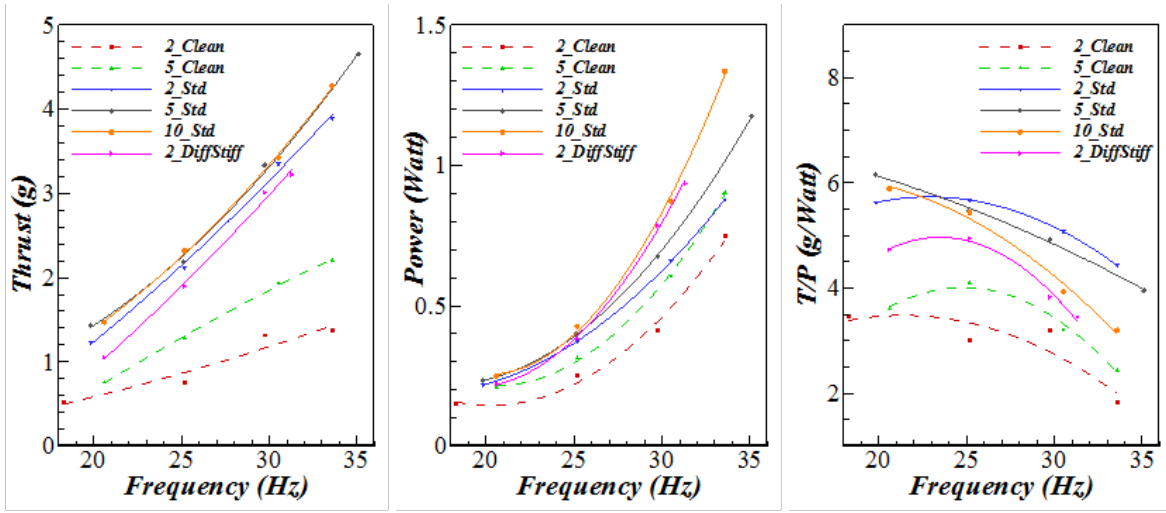


Figure 5: Performance plots for wings with different flexibility. Left: Thrust; Middle: Power consumption; Right: Thrust to power consumption ratio.

### 3.3 Wind Tunnel Test

The flapping performance for the hovering case has been experimentally investigated as discussed in the previous section. This section will examine the flapping performance within incoming flow velocity, representing the forward flight regime. The calibrated wind speed is set at 2m/s, 3m/s and 4m/s. For each velocity, the angle of attack changes from 20° to 40° with an increment of 10°.

Fig. (6) shows the lift and thrust with varying frequencies and free stream velocities. The horizontal and vertical dash lines represent the weight of ‘Delfly Micro’ (3.07g) and level flight at a constant velocity (zero thrust), respectively. These two lines segment the figure into four parts, where the right top quarter is the region where ‘Delfly Micro’ has more lift than its weight and positive thrust for flight. The crossing point of the two lines is the equilibrium level flight point of ‘Delfly Micro’, where the lift equals the weight and zero thrust is zero (actually, this is the total horizontal force, so thrust minus drag in the conventional concept of aeronautics). For the investigated range of flapping frequency and angle of attack, some points fall within the flight operation region for  $U = 2$  m/s and 3 m/s, but this is not the case for  $U=4$ m/s. This suggests that ‘Delfly Micro’ may not be able to fly faster than 4m/s. Moreover, the level flight points can be found in Fig. (6(Left)) that ‘Delfly Micro’ can fly at 2m/s with flapping frequency of 28Hz and 36° angle. By increasing the frequency to 34Hz ‘Delfly Micro’ is able to fly up to 3m/s with angle of 25°, depicted in Fig. (6(Middle)).

In view of the lift and thrust data plotted in Fig. (6), the ‘Delfly Micro’ can fly up to 3 m/s. In order to determine the required motor performance, the power consumption versus flapping frequency at different angle of attack is plotted in Fig. (7), for  $U=2$  m/s. Noted that at the operation point around 30Hz, the motor should be powerful enough to produce 1 Watt power. In the design stage, the driving system including motor, controller, receiver and battery should be able to output 2 Watts power for reliable flight.

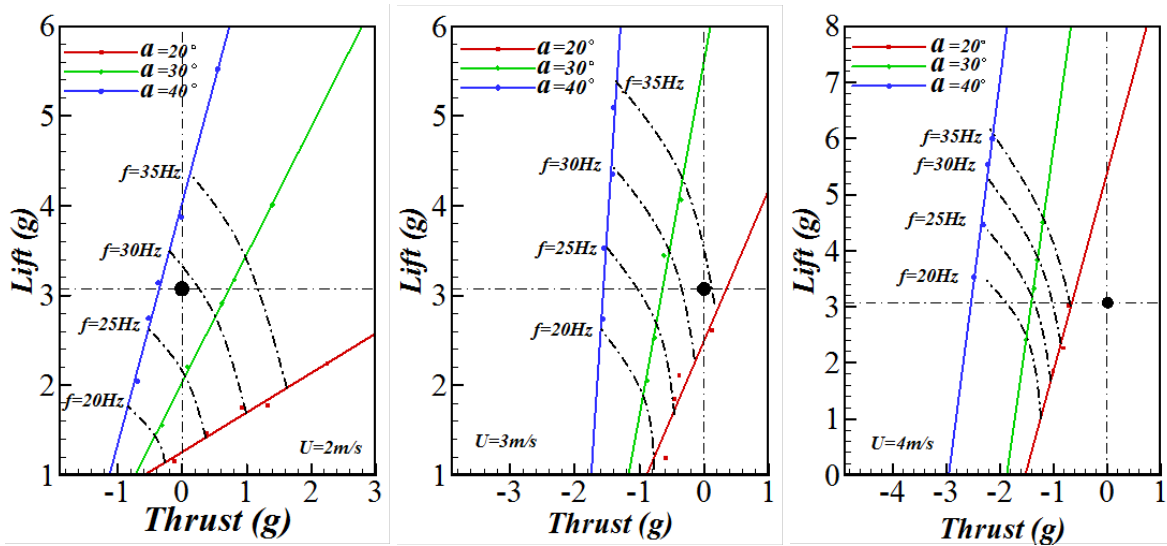


Figure 6: Lift and Thrust with varying incoming flow velocity. Left:  $U=2\text{m/s}$ ; Middle:  $U=3\text{m/s}$ ; Right  $U=4\text{m/s}$ .

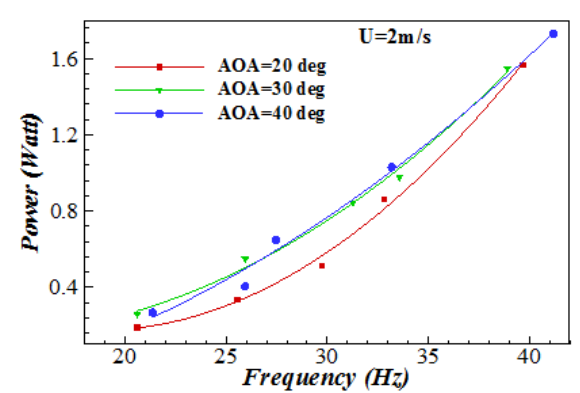


Figure 7: Power Consumption versus Frequency,  $U=2\text{m/s}$ .

## 4 Conclusion

There are two thrust peaks in one flapping period, and the peaks' location shifts with respect to flexibility and flapping frequency. The flexibility of the wing significantly influences the flapping performance. More rigid wings can produce more forces during flapping, however, they are more energy consuming. The standard wing built by 2m Mylar membrane possesses the best performance of the investigated wings, with slight scarfing in thrust compared with the wings made from 5 m and 10 m thickness Mylar. Wind tunnel tests define the initial flight envelop, and suggest that the 'Delfly Micro' can guarantee a level flight around  $3\text{m/s}$  with  $34\text{Hz}$  flapping frequency and  $25^\circ$  angle

of attack. Based on the results, the calibrated driving system on ‘Delfly Micro’ should be powerful enough to produce 2 Watts power in further optimization. Further testing will be performed on the instantaneous deformation of the wing. Also the interaction between flapping wings and the tail has to be investigated for optimizing the tail position and mount angle.

## Acknowledgement

This work has been supported by the Netherlands Technology Foundation (STW, project number 11023) and the China Scholarship Council (CSC). Thanks to the technical assistance from Stefan Bernardy in the Low Speed Lab of Delft University of Technology.

## References

- [1] G C H E de Croon, M A Groen, C De Wagter, B Remes, R Ruijsink, and B W van Oudheusden. Design, aerodynamics and autonomy of the delfly. *Bioinspiration and Biomimetics*, 7(2):025003, 2012.
- [2] M. Percin Y. Hu B. W. van Oudheusden B. Remes and F. Scarano. Wing flexibility effects in clap-and-fling. *International Journal of Micro Air Vehicles*, 3(4):217–228, 2011.
- [3] M. Percin M.Eisma B. W. van Oudheusden B. Remes R.Ruijsink and R. deWagter. Flow visulation in the wake of the flapping-wing mav ‘delfly ii’ in forward flight. *at the 30th AIAA Applied Aerodynamics Coference*, pages AIAA–2012–2664, 2012.
- [4] W.Tay H.Bijl and B. W. van Oudheusden. Analysis of biplane flapping flight with tail. *at the 30th AIAA Applied Aerodynamics Coference*, pages AIAA–2012–2968, 2012.
- [5] B.Bruggeman. Improving flight preformance of delfly ii in hover by improving wing design and driving mechanism. Master’s thesis, Faculty of Aerospace Engineering, Delft University of Technology, 2010.
- [6] T. Weis-Fogh. Quick estimates of flight fitness in hovering animals, including novel mechanisms for lift production. *Journal of Experimental Biology*, 59(1), 1973.
- [7] J.Eisma. Flow visualization and force measurements on a flapping-wing mav delfly ii in forward flight configuration. Master’s thesis, Faculty of Aerospace Engineering, Delft University of Technology, 2012.